



# A novel method for the immobilization of urease on phosphonate grafted iron oxide nanoparticle

Banalata Sahoo, Sumanta Kumar Sahu, Panchanan Pramanik\*

Department of Chemistry, Indian Institute of Technology, Kharagpur, 721302, W. B., India

## ARTICLE INFO

### Article history:

Received 11 October 2010

Received in revised form

28 December 2010

Accepted 4 January 2011

Available online 7 January 2011

### Keywords:

Magnetic nanoparticles

Enzyme immobilization

Urease

Phosphonomethyl iminodiacetic acid

## ABSTRACT

The development of simple and reliable technique for the immobilization of enzymes is an important part of biotechnology. We demonstrate herein the modification of magnetic nanoparticles and its use in the immobilization of the urease enzyme. Magnetite particles were prepared by simple co-precipitation method in aqueous medium and then subsequently coated with phosphonomethyl iminodiacetic acid. Urease was immobilized on the magnetic nanoparticles through a carbodiimide reaction. Surface functional groups and surface composition were analyzed by Fourier transform infrared (FTIR) spectroscopy and thermo gravimetric analysis (TGA), respectively. The structural characteristics of the powders were studied by XRD. These modified nanoparticles were characterized by dynamic light scattering (DLS) and high resolution transmission electron microscopy (HRTEM). Vibration sample magnetometry (VSM) measurements showed the superparamagnetic nature of the particles at room temperature. The catalytic activity of the immobilized urease was comparable to that of the free enzyme in solution. The immobilized urease exhibited excellent catalytic activity over six times successive reuse as well as the stability. By using immobilization technique on this magnetic nanoparticle it is easy to isolate product from reaction mixture enabling to control the reaction and simultaneously lowers the cost of enzyme.

© 2011 Elsevier B.V. All rights reserved.

## 1. Introduction

Metal oxide nanoparticles, with their potential applications in the fields of physics, chemistry, biology, and medicine have attracted increasing research attention from the past decades because of their interesting physical and chemical properties. In the recent years, nanosized iron oxide particles have been paid considerable attention in the fields of biological applications [1–5]. Applications of these magnetic iron oxide nanoparticles not only cover traditional electrical, optical, magnetic areas but also expand applications in biotechnologies. Magnetic nanoparticles have been widely used in the immobilization of enzymes [6], immunoassay [7], bioseparation [8], biosensor [9], targeted drug delivery [10], and environmental analysis [11]. It is cheap, non-toxic, biocompatible, and easy to prepare. The surface properties of magnetic nanoparticle allow to functionalize magnetic nanoparticles by various functional groups for a range of applications. Although there are several reports on generating water soluble magnetic nanoparticles, most of methods produce poor dispersibility in aqueous solutions. Therefore, using hydrophilic molecules to modify the surface of magnetic nanoparticles becomes a necessary requirement before their use in biological systems.

Enzymes are versatile biocatalyst that control specific chemical reactions effectively *in vivo* and *in vitro* [12]. To make enzymes cost-effective and long lived, various supports have been utilized to immobilize enzymes through polymer membranes [13,14], silica [15,16], chitosan–siloxane hybrids [17] a zeolites [18], and molecular sieves [19,20]. Immobilization of enzymes onto solid supports is a popular principle for a wide range of applications because of their low cost, recyclability, fast product separation, improvement in enzyme stability, and to make catalytic properties intact [21]. Nanomaterials have potential to serve as superior support for enzyme immobilization due to their large surface-to-volume ratios in comparison with traditional macroscale materials, where the reduction of substrate size may induce the deactivation and the desorption of enzymes in the processes of enzymatic reactions [22]. Magnetic nanoparticles have a wide promise to immobilize enzyme on its surface not only to perform better than micrometer-sized resins or beads used in enzyme immobilization but also faster separation by external magnetic field. Moreover the efficient separation of the suspended small solid enzyme carriers from product using an external magnetic field is therefore of immense interest [23].

Urease is a highly efficient catalyst for the hydrolysis of urea. Urease converts urea to ammonia and carbon dioxide. Urea is the main toxic metabolic products, and removal of this excess is a major problem for patients suffering from renal failures [24]. The enzyme is found in a variety of bacteria, fungi, and plants thus playing

\* Corresponding author. Tel.: +91 9475196288; fax: +91 3222255303.  
E-mail address: [banalata99@gmail.com](mailto:banalata99@gmail.com) (P. Pramanik).

an important role in the circulation of nitrogen in nature. The applications of urease in biotechnology are urea content analysis in blood, urine, alcoholic beverages, natural water, and environmental wastewaters. The most effective way of removing urea from aqueous solutions is the utilization of immobilized urease as no efficient adsorbents available. The urease enzyme is utilized for homogeneous generation of  $\text{CO}_2$  and  $\text{NH}_3$  for various analytical applications. However, there is no simple means to remove enzyme from reaction mixture. In this regard urease tagged magnetic nanoparticle would be very effective to replace pure enzyme and after the reaction magnetic enzyme can be separated from reaction mixture by external magnetic field. In this principle iron oxide nanoparticles with superior magnetic properties hold best support material for enzyme immobilization. Many polymeric materials have been used for urease immobilization and their applications in analytical and biomedical fields are well studied [25–27]. A significant focus on current research is to replace polymer support and develop surface functionalized iron oxide nanoparticles to immobilize urease. As the support of enzymes immobilization, magnetic nanoparticles are of great interest and the use of magnetic nanoparticles for enzyme immobilization has been widely investigated [28–31]. To the best of our knowledge, the immobilization of urease onto phosphonate grafted magnetic nanoparticle is not established.

Recently, we have reported the practical implementation of phosphonate stabilized magnetic nanoparticles in various biological applications [32–34]. In this work we have modified phosphonate conjugated iron oxide nanoparticles of approximately 20 nm for immobilization of urease. Our main aim is the development of a facile, economical, and simple strategy for the synthesis of monodisperse hydrophilic superparamagnetic nanoparticles for immobilization of enzyme. The surface of iron oxide nanoparticles is functionalized with N-phosphonomethyl iminodiacetic acid (PMIDA) as a ligand. In this contribution, we report a simple and low-cost route to immobilize urease on superparamagnetic nanoparticles through carbodiimide reaction. Surface coating of the ligand has been established by FTIR, thermal analysis, and XPS analysis. The structural purity of the iron oxide nanoparticle has been investigated by XRD studies. These PMIDA modified magnetic nanoparticles are characterized in terms of their size distribution by dynamic light scattering (DLS) and high resolution transmission electron microscopy (HRTEM). Urease is immobilized on the magnetic nanoparticles surface, the detail activity and kinetic behavior of the immobilized urease have been studied at different conditions. To our knowledge, this PMIDA functionalized magnetic nanoparticle is used for the first time as a support material for enzyme immobilization.

## 2. Materials and methods

### 2.1. Materials

Urease (From Jack bean, activity 50,000–100,000 units/g solid) was obtained from Sigma Chemicals, USA.  $\text{FeCl}_3$  (anhydrous) and  $\text{FeSO}_4 \cdot 6\text{H}_2\text{O}$  were procured from Merck, Germany. N-phosphonomethyl iminodiacetic acid (PMIDA) and urea were obtained from Aldrich Chemicals, USA. Ethylenediaminetetraacetic acid (EDTA), sodium tungstate ( $\text{Na}_2\text{WO}_4 \cdot 2\text{H}_2\text{O}$ ), 1-[3-(dimethylamino) propyl]-3-ethylcarbodiimide hydrochloride (EDC), were obtained from Merck. All the chemicals were used without further purification. The water used in this work was Millipore water. Nessler's reagent was prepared as usual procedure reported on Inorganic Practical Analysis by Vogel.

### 2.2. Synthesis of magnetite nanoparticles

Magnetic nanoparticles were synthesized according to our reported procedure [35]. In a 100 ml three necked flask equipped with a mechanical stirrer were taken 0.324 g of  $\text{FeCl}_3$  and 0.278 g of  $\text{FeSO}_4 \cdot 6\text{H}_2\text{O}$  in 40 ml of absolutely deoxygenated Millipore water under argon flow. 5 ml of  $\text{NH}_3$  (25%) solution was added into it drop wise over a period of 15 min during which black precipitates formed. The reaction mixture was stirred for 30 min at  $70^\circ\text{C}$ . Then the black particles were separated and washed 5 times with Millipore water by magnetic concentrator. In the next step the nanoparticles were dispersed in Millipore water thoroughly by using ultrasonic probe (Misonix 3000) with micro tip for 30 min at  $37^\circ\text{C}$ . For surface modification on magnetite nanoparticles  $\text{Fe}_3\text{O}_4$  and PMIDA were taken 1:1 molar ratio in alkaline medium which was maintained pH 8.0. This solution was again sonicated for 20 min. The particles were separated magnetically and washed five times with water followed by ethanol and dried in vacuum. Few drops of the suspended particles in water were acidified with dilute acetic acid (pH was maintained 4–5) and further dispersed in 10 ml of Millipore water by ultrasonication and was activated by EDC, then the reaction mixture was stirred for 3–4 h. The EDC activated magnetic nanoparticles were washed three times with Millipore water in order to remove unreacted EDC. The magnetic nanoparticles were recovered by magnetic separation using a permanent magnet. Finally the above EDC activated carboxyl terminated nanoparticles was treated with enzyme as mentioned below.

### 2.3. Conjugation of urease on magnetite nanoparticles

10 mg of above functionalized magnetic nanoparticles were treated with 2 mg urease containing 8 ml. Phosphate buffer (0.01 M) having pH 7.4 and the resulting solution was stirred for 12 h at  $4^\circ\text{C}$ . After 12 h enzyme tagged magnetic nanoparticles were washed five to six times with PBS (pH 7.4). The supernatant after immobilization was collected to determine the amount of enzyme bound to the magnetic nanoparticle surface. The urease conjugated with  $\text{Fe}_3\text{O}_4$ -PMIDA producing magnetic enzyme.

### 2.4. Urease activity assay and protein determination

The activities of the urease (free and immobilized) were determined using Nessler's method [36]. After the immobilization of urease, the magnetic nanoparticles were retained by a magnet, and the UV absorption value of the supernatant solution was mea-

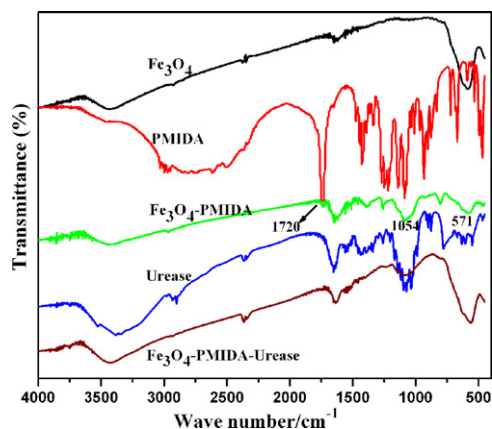
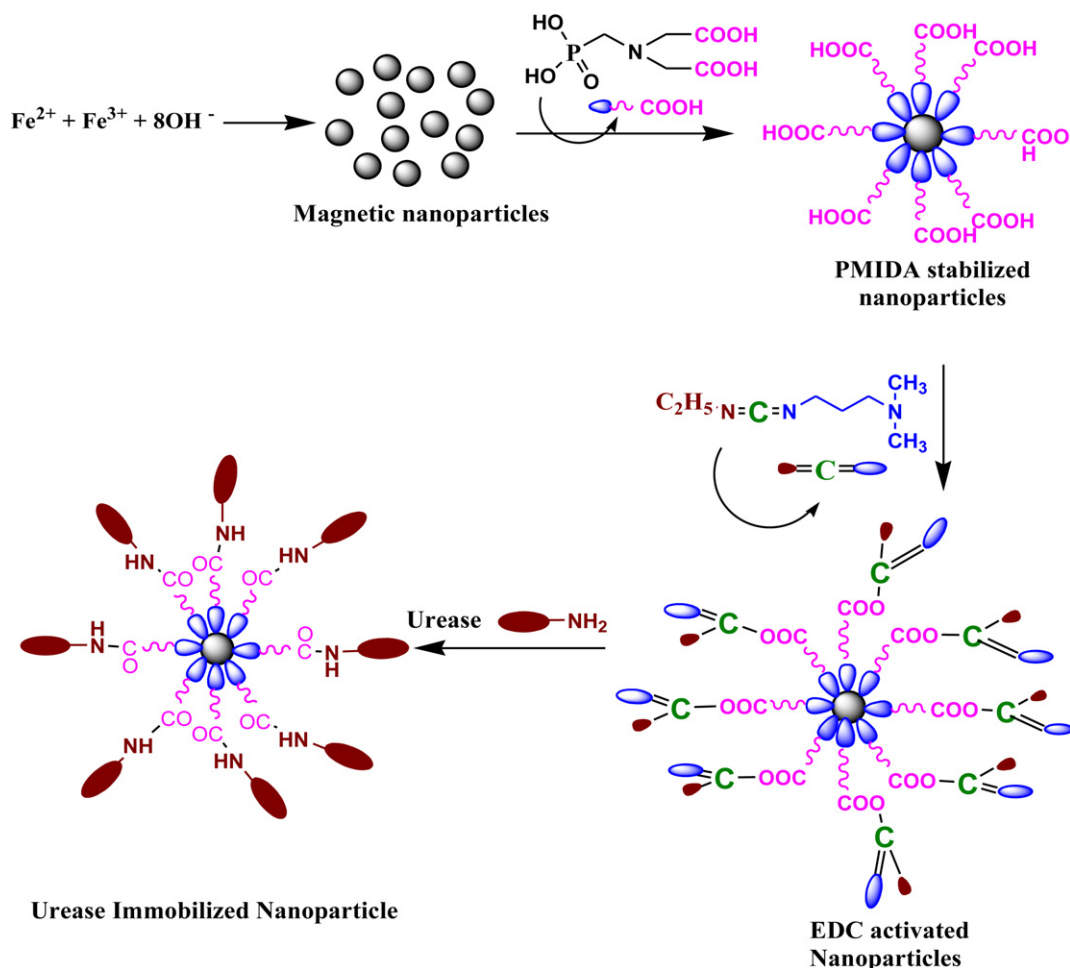


**Fig. 1.** FTIR spectra of  $\text{Fe}_3\text{O}_4$  nanoparticles, PMIDA,  $\text{Fe}_3\text{O}_4$  functionalized PMIDA nanoparticles, native urease and immobilized urease on  $\text{Fe}_3\text{O}_4$ -PMIDA nanoparticles.



**Scheme 1.** Systematic procedure for the immobilization of urease on the PMIDA functionalized iron oxide nanoparticle.

sured at 480 nm to calculate the activity of immobilized urease on the magnetic nanoparticles. The amount of protein bound to the nanoparticle surface was calculated in UV–Vis spectrophotometer using a standard curve of various concentrations of urease versus absorbance at 280 nm.

### 2.5. Characterization

The phase formation and crystallographic state of uncoated as well as functionalized magnetic nanoparticles were determined by Phillips PW 1710 X-ray diffractometer with Ni-filtered  $\text{Co-K}\alpha$  radiation ( $\lambda = 1.79 \text{ \AA}$ ). Presence of surface functional groups was investigated by FTIR spectroscopy. The samples were prepared in KBr medium in the range  $400\text{--}4000 \text{ cm}^{-1}$  with a model Thermo Nicolet Nexux FTIR (model 870). The surface compositions of the different nanoparticle preparations were obtained by analyzing XPS data using an Al  $\text{K}\alpha$  excitation source in an ESCA-2000 Multilab apparatus (VG microtech). Thermal analysis was done with a thermal analyzer (Pyris Diamond TG/DTA) with a heating rate  $8^\circ\text{C}/\text{min}$  with in temperature range  $50\text{--}850^\circ\text{C}$ . The size and morphology of the nanoparticles were observed using a Phillips CM 200 transmission electron microscope (TEM) with an acceleration voltage 200 kV. The nanoparticles were thoroughly dispersed in water by ultra-sonication and placing a drop of solution on the carbon coated copper grid. The hydrodynamic size of the particle was measured by dynamic light scattering (DLS) techniques, using a Brookhaven 90 Plus particle size analyzer. The laser light of wavelength ( $\lambda = 660 \text{ nm}$ ) was scattered with an angle  $\theta = 90^\circ$  at  $27^\circ\text{C}$

placing the dispersion in a polystyrene cuvette. Magnetic measurements were performed using vibration sample magnetometry.

### 3. Results and discussion

Magnetic nanoparticles are prepared by co-precipitation from  $\text{Fe}^{2+}$  and  $\text{Fe}^{3+}$  using  $\text{NH}_4\text{OH}$  solution. Particles are modified with PMIDA for stable aqueous magnetic dispersion. This PMIDA is an effective coupling agent containing one phosphonate and two carboxyl functions per molecule. This phosphonate groups strongly anchor the nanocrystal surface, the free carboxyl functions on the outer surface induce electrostatic repulsion between the nanocrystals, which generates an exceptionally stable ferrofluid. Then this carboxyl decorated magnetic nanoparticles are activated by EDC and then conjugated with urease by simple carbodiimide reaction. Scheme 1 illustrates the detail synthetic procedure for PMIDA functionalized magnetic nanoparticles and immobilization of urease.

The conjugation of PMIDA onto the  $\text{Fe}_3\text{O}_4$  surface is established from Fourier transform infrared spectroscopy. The comparison of FTIR spectrum of pure magnetic nanoparticles, PMIDA, PMIDA modified magnetic nanoparticles ( $\text{Fe}_3\text{O}_4\text{-PMIDA}$ ), urease and immobilized urease ( $\text{Fe}_3\text{O}_4\text{-PMIDA-urease}$ ) is shown in Fig. 1. For pure magnetic nanoparticles exhibit a strong band at  $571 \text{ cm}^{-1}$ , characteristic of the Fe–O vibration correlated to the magnetic core and the broad band around  $3300 \text{ cm}^{-1}$ , indicative of the presence of –OH groups on the nanoparticle surface. After modification of PMIDA on the nanoparticles surface a significant decrease in the

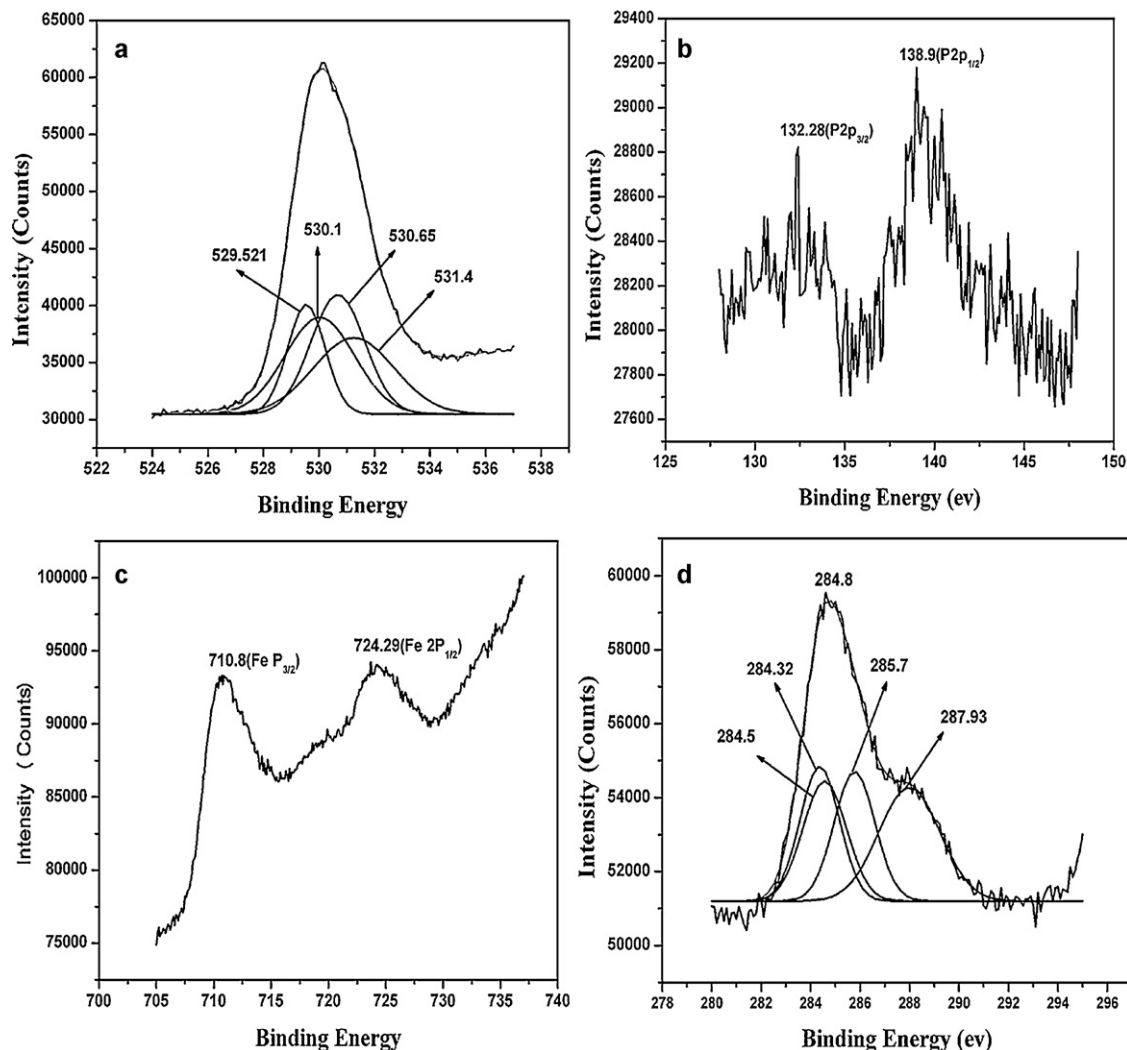


**Fig. 2.** X-ray photoelectron spectra of PMIDA modified magnetic nanoparticles using Al K $\alpha$  source. (a–d) High-resolution O1s, P2p, Fe2p, and C1s spectra with fitted curves.

intensity of the band at  $571\text{ cm}^{-1}$  is observed which indicates the adsorption of phosphonic acids on the magnetite surface. A broad peak at  $1054\text{ cm}^{-1}$  accounts for M–O–P and P=O stretching bands superimposed on one another. The typical vibrations of a  $-\text{CO}_2\text{H}$  group ( $1720\text{ cm}^{-1}$ ) appear in the corresponding FTIR spectrum. After conjugation with urease, the spectrum of the resultant nanoparticles  $\text{Fe}_3\text{O}_4$ –PMIDA–urease show the characteristic bands at  $571, 1635\text{ cm}^{-1}$  ( $-\text{CONH}$  amide band) and  $1554\text{ cm}^{-1}$  ( $-\text{NH}$  amide band). From this absorption spectra it is confirmed that the successful conjugation of urease on the  $\text{Fe}_3\text{O}_4$ –PMIDA nanoparticles.

X-ray photoelectron spectroscopy analysis is further used to validate the successful PMIDA functionalized magnetite nanoparticles (Fig. 2). The high resolution O1s spectrum (Fig. 2a) of PMIDA-coated magnetite displayed peaks at 529.52, 530.1, 530.6, and 531.4 eV, which corresponded to oxygen being present in four different environments as P–O, C–O, Fe–O, and O–H. The P2p spectrum (Fig. 2b) exhibited two peaks at 132.26 and 138.9 eV corresponding to P2p $_{3/2}$  and P2p $_{1/2}$ , respectively. The Fe2p doublet with binding energy values of 710.8 and 724.29 eV (Fig. 2c) implied the presence of Fe–O bonds, typical for magnetite. Furthermore, the high-resolution C1s spectrum (Fig. 2d) displayed four peaks at 284.32, 284.5, 285.7 and 287.93 eV, attributed to C–C, C=O, NH–C=O, and C=O (typical of ester/carboxylic acid).

Fig. 3 shows the XRD patterns for pure  $\text{Fe}_3\text{O}_4$ , and PMIDA conjugated  $\text{Fe}_3\text{O}_4$  nanoparticles. The characteristic peaks at  $2\theta = 35.45^\circ$ ,

$41.55^\circ$ ,  $50.53^\circ$ ,  $63.7^\circ$ ,  $67.64^\circ$ , and  $74.36^\circ$  for pure  $\text{Fe}_3\text{O}_4$  nanoparticles, which were marked respectively by their indices (220), (311), (400), (422), (511), and (440), were also observed for  $\text{Fe}_3\text{O}_4$ –PMIDA nanoparticles. This revealed that the surface modification and conjugation of the  $\text{Fe}_3\text{O}_4$  nanoparticles do not lead to their phase change. The  $d$  values correspond to that of inverse spinel magnetite [ $\text{Fe}_3\text{O}_4$ ] (JCPDS card no. 85-1436). The broadening

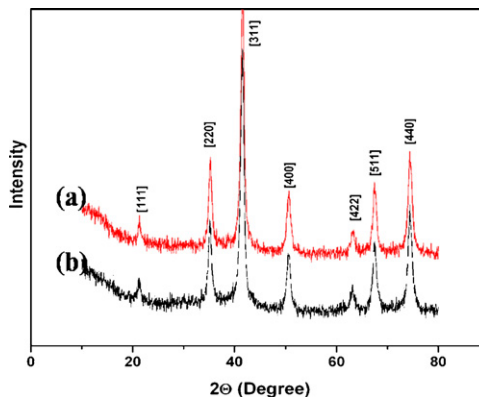


**Fig. 3.** X-ray diffraction patterns for pure  $\text{Fe}_3\text{O}_4$  nanoparticles (a) and PMIDA functionalized  $\text{Fe}_3\text{O}_4$  nanoparticles (b).



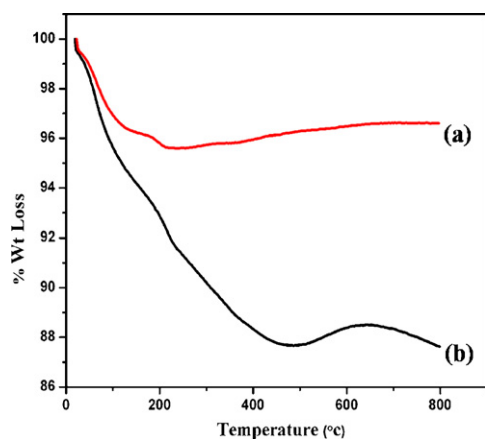


**Fig. 4.** Weight loss analysis from TG curves of (a) as prepared  $\text{Fe}_3\text{O}_4$  and (b) PMIDA functionalized  $\text{Fe}_3\text{O}_4$  nanoparticles.

of each peak in XRD mean crystallite size was calculated by applying Scherrer's equation:  $D = 0.9\lambda / \beta \cos \theta$ , where  $D$  is the average diameter in  $\text{\AA}$ ,  $\beta$  is the broadening of the diffraction line measured at half of its maximum intensity in radians,  $\lambda$  is the wavelength of the X-rays and  $\theta$  is the Bragg diffraction angle. The mean crystallite size was found to be around 20 nm.

Thermal analysis was performed to confirm the coating formation on the surface of the magnetite. Fig. 4 shows comparative weight loss for uncoated iron oxide and  $\text{Fe}_3\text{O}_4$ -PMIDA. In the case of uncoated magnetic nanoparticles the weight loss between 50 and

$150^\circ\text{C}$  is due to loss of physically adsorbed water molecules. The weight loss between 150 and  $250^\circ\text{C}$  is presumably due to the loss of surface hydroxyl groups. In the case of  $\text{Fe}_3\text{O}_4$ -PMIDA the weight loss at  $50$ – $150^\circ\text{C}$  is due to the loss of physically adsorbed water on the surface. The weight loss in the second regime (9%) corresponds to the decomposition of the adsorbed phosphonic acid coupling agent.

The typical HRTEM images and particle size distributions of the PMIDA coated magnetic nanoparticles and urease immobilized on the same nanoparticles are shown in Fig. 5. From the figures, PMIDA stabilized magnetite nanoparticles are well dispersed. The nanoparticles are narrow size distribution with a mean average size of 17.5 nm and after enzyme immobilization on the same nanoparticles are almost uniform sizes. The hydrodynamic diameter of the PMIDA modified magnetic nanoparticles is determined by DLS technique. Here we have observed that the size measured by the DLS is higher than the TEM measurement. It is due to the thin phosphono coating formed around small aggregates of the magnetite particles. The formation of small aggregates of magnetite nanoparticles results from the magnetic dipolar interaction among the particles. The thin layer coating on the nanoparticles surface could reduce the magnetic dipolar interaction and promote the stability of magnetite nanoparticles. From DLS measurement the average diameter of PMIDA coated iron oxide is 55–75 nm and after urease immobilization particle size is increased from 80 to 100 nm. This reveals that the conjugation of urease on the nanoparticles surface.

Plots of magnetization versus magnetic field at 300 K for  $\text{Fe}_3\text{O}_4$  and enzyme immobilized PMIDA conjugated  $\text{Fe}_3\text{O}_4$  nanoparticles

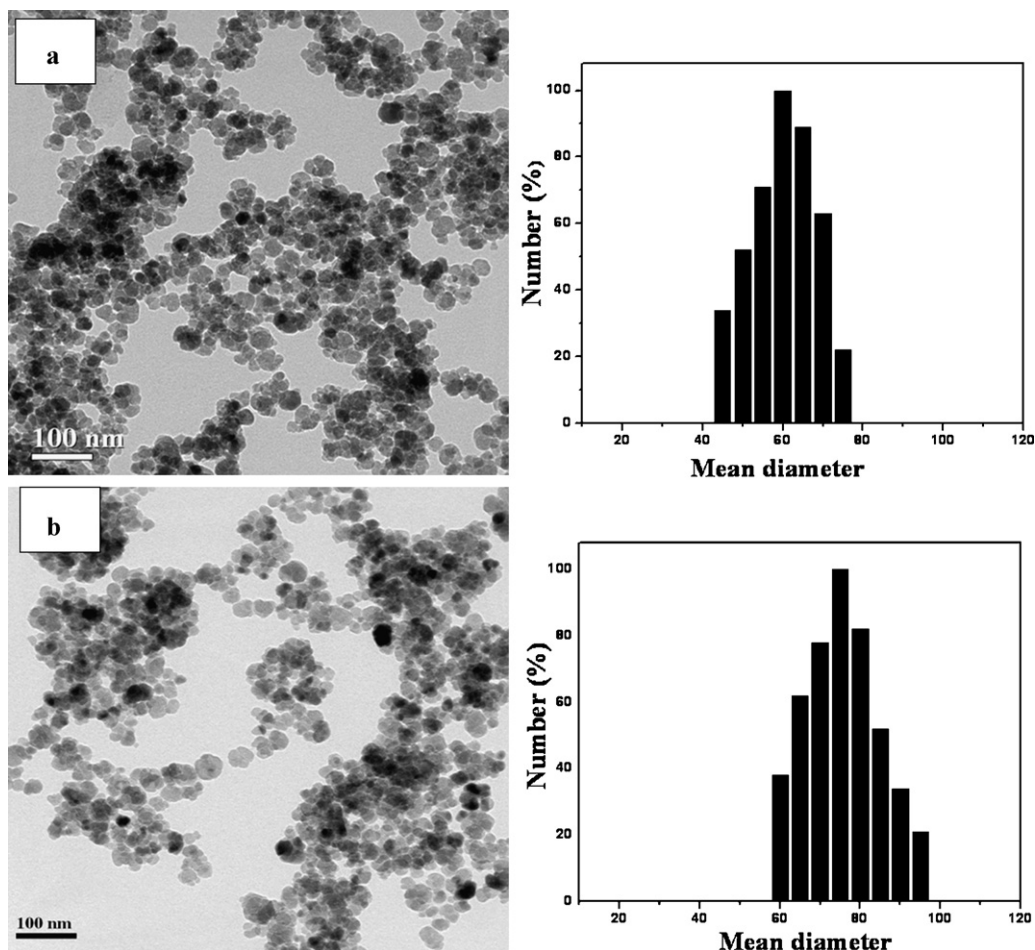


**Fig. 5.** TEM micrographs and DLS size distributions of  $\text{Fe}_3\text{O}_4$ -PMIDA nanoparticles before (a) and after (b) conjugation with urease.

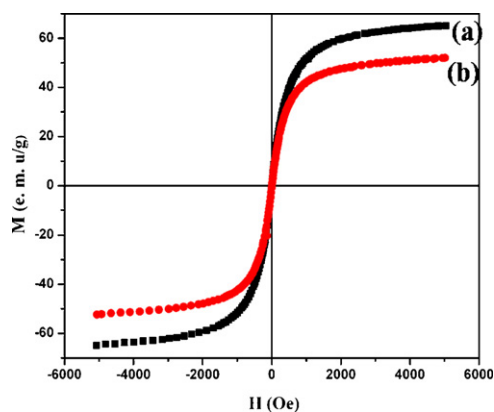
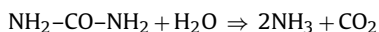


**Fig. 6.** Magnetization curves of (a) pure  $\text{Fe}_3\text{O}_4$  and (b) PMIDA conjugated  $\text{Fe}_3\text{O}_4$  nanoparticles at room temperature.

are illustrated in Fig. 6. The saturation magnetizations are found to be 65.4 emu/g for bare magnetic nanoparticles and 48.3 emu/g for enzyme immobilized PMIDA conjugated  $\text{Fe}_3\text{O}_4$  nanoparticles. Moreover, the magnetization curves in two cases exhibit nearly zero remanence, which proves the existence of the superparamagnetic character. This reduction in  $M_s$  could be partially contributed by the diamagnetic organic coating and defect in crystal. In addition to this, the disordered structure and incomplete crystallization at the interface could be a cause for decrease in effective magnetization. These magnetically active properties of the PMIDA conjugated  $\text{Fe}_3\text{O}_4$  nanoparticles render them very susceptible to magnetic fields and therefore make the solid and liquid phases separate easily.

Urease activity is determined through the hydrolysis experiment of urea and subsequent measurement in UV–Vis spectrometer. The known hydrolysis reaction of urea with enzyme urease is



The specific activity of conjugated urease is predicted through the determination of ammonia concentration using Nessler's reagent. The final product exhibits a brown color whose absorbance at 480 nm is proportional to the ammonia concentration. The activity of the urease was calculated from the production rate of  $\text{NH}_3$  in a period of 30 min. The enzymatic activity of urease immobilized on magnetic nanoparticle is studied by plotting the graph between the hydrolysis rate of urea versus the concentration of product formed at room temperature which is shown in Fig. 7. From figure it is depicted that urea is catalytically hydrolysed by

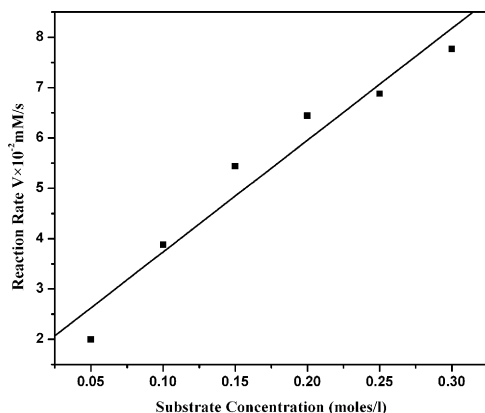


**Fig. 7.** Variation of reaction rate with substrate concentrations of immobilized urease.

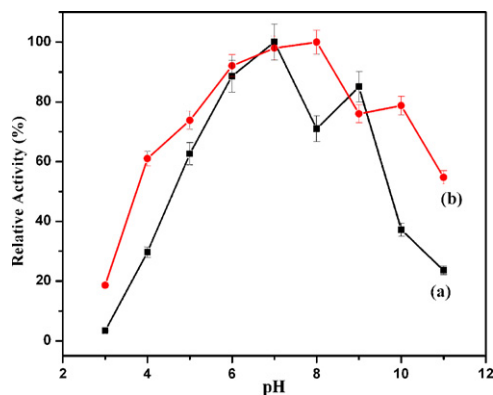


**Fig. 8.** Optimum pH of (a) native urease and (b) immobilized urease onto PMIDA coated magnetic nanoparticles.

immobilized urease. On adding excess substrate concentration and keeping it for prolonged period does not depict any more hydrolysis which means the active site of the enzyme becomes fully saturated with substrate. The specific activity of urease is expressed in mM ammonia liberated per minute while the relative activity is taken as the amount of ammonia (mM) liberated expressed in percentage. In the present investigation, urease immobilized on PMIDA modified magnetic nanoparticles retained 57% of its specific activity. The amount of urease immobilized on PMIDA modified magnetic nanoparticles was observed by increase with increasing enzyme concentration for each particle concentration. The amount of urease immobilized on PMIDA modified magnetic nanoparticles was observed maximally 2.4 mg protein/10 mg particle.

The effect of pH on urease activity has been investigated by varying the pH of buffer from 3.0 to 11.0. The pH dependence of enzymatic activity is presented in Fig. 8. The native urease shows its maximum activity at pH 7.0 whereas the immobilized enzyme shows its maximum activity at pH 8.0. However, the immobilized urease shows almost equal catalytic activity varying pH range from 3.0 to 8.0. On the other hand the relative catalytic activity was decreased at pH higher and lower than 7.0. This shows the immobilization enhances the stability of enzyme at broader pH. This result indicates that the immobilized enzyme has greater stability at different pH ranges. Immobilized urease shows better activity in acidic pH as compared to free urease and the catalytic activity of immobilized enzyme is retained. This is due to the immobilized enzyme is less sensitive to pH changes than that of free urease. However by immobilizing enzyme on magnetic nanoparticles surface we have reused several times. According to Gabrovská et al. [37], the maximum activity for both free and immobilized enzyme was at pH 5.8. With rise in pH from 5.8 to 7.0 the catalytic activity was decreased for urease immobilized on polyacrylonitrile–chitosan membrane. Bayramoglu et al. [24] observed the maximum urease activity at pH 6.5. The retention of activity of immobilized enzyme on magnetic nanoparticles at different pH might be caused due to rigid structure formation through covalent immobilization which seems to be one of the most promising possibilities to improve enzyme stability.

Thermal stability of immobilized and native urease is compared by measuring their activities at various temperatures ranging from 30 to 80 °C shown in Fig. 9. With increase in temperature the percentage of decrease in the catalytic efficiency of native urease is reasonable but immobilized enzyme shows increasing in catalytic activity. At 80 °C, the immobilized urease retained its activity whereas the native urease lost 90% of its original activity. Hence, these results showed that immobilized enzyme has better thermal resistance as compared to its native counterpart. The enhancement of thermal stability of immobilized enzyme is attributed due to covalent bonding between carboxyl decorated iron oxide

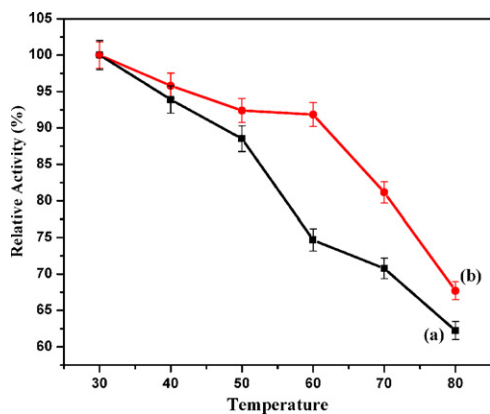


Fig. 9. Optimum temperature of (a) native urease and (b) immobilized urease onto PMIDA coated magnetic nanoparticles.

and urease, which may restrict the conformational change of urease through heating. The improved thermal enzymatic stability through binding on magnetic nanoparticle has been ascribed to higher hydration strength of the enzyme on nanoparticle. The presence of special water structuring properties of hydroxyl group on nanoparticle which prevents the denaturation of enzyme. We conclude that this behavior is probably due to constraint induced by covalent bonds that hinder denaturing by molecular relaxation [38].

The stability of enzyme on magnetic nanoparticle is determined by checking its activity in six continuous experiments performing every five days interval for a total period of one month. From Fig. 10 it is observed that the immobilized enzyme shows up to 70% of relative activity after five times reuse. It means the immobilized enzyme retains its catalytic activity for repeated use. From figure we conclude that the immobilized enzyme is very stable. But free enzyme cannot be reused and recycled for next subsequent catalytic experiment.

The immobilized urease is stored in 0.01 M phosphate buffer saline at pH 7.4 at 4 °C for 45 days. The activity is checked at regular 5 days interval which we have already discussed in our previous experiment. The immobilized enzyme retains its activity even after 6 times of repeated uses through the isolation of magnetic enzyme by external magnetic field. The strong binding of urease on the surface of magnetic nanoparticles by covalent attachment enhances the stability of enzyme. The storage stability of both native urease and free urease is investigated. Both native enzyme and immobilized enzyme are stored at 4 °C. It is indicated that the immobilized

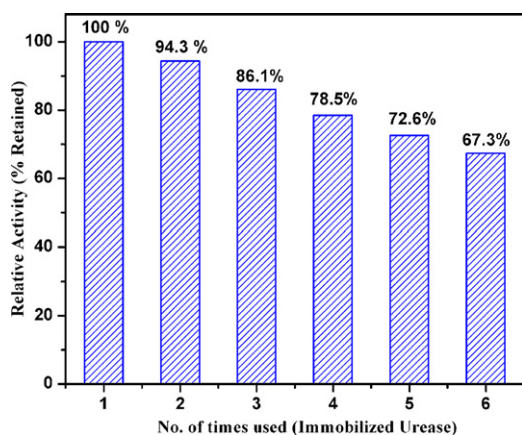


Fig. 10. Reusability of the immobilized urease on PMIDA coated magnetic nanoparticles in repeated batch hydrolysis of urea.

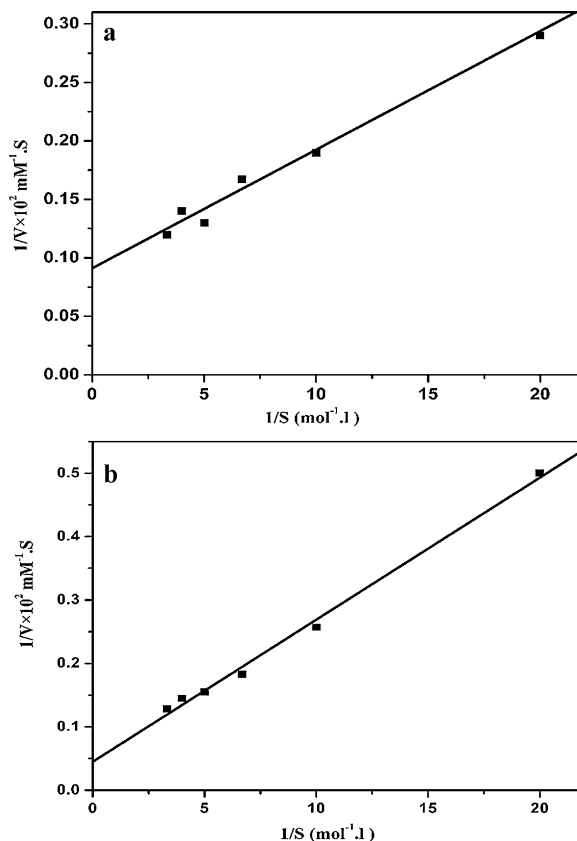


Fig. 11. Lineweaver–Burk plot for the maximum hydrolysis rate ( $V_{\max}$ ) of native (a) and immobilized urease (b) at the room temperature.

enzyme shows better storage stability for a longer period of time as compared to native urease. The immobilized urease retained up to 70% activity over a period of 45 days. In contrast free enzyme lost all its catalytic activity after the same time period.

The Michaelis constant is determined from the Lineweaver–Burk plot which is shown in Fig. 11. Both free and immobilized enzyme activity are determined 32 °C in 0.01 M phosphate buffer saline at pH 7.4. The graph is plotted taking different substrate concentrations and their corresponding reaction rate. The reciprocal of substrate concentration ( $1/S$ ) is plotted against the reciprocal of reaction rate ( $1/V$ ) according to the following equation:

$$\frac{1}{V} = \frac{K_m}{V_{\max}} + \frac{1}{V_{\max}}$$

In both the cases the graphs are linear indicating free and immobilized enzyme obey Michaelis–Menten enzyme kinetics and the kinetics data is fitted with Michaelis–Menten equation. The intercept of the straight-line gives the value of the inverse of maximum hydrolysis rate ( $1/V_{\max}$ ) of urea, whereas the slope gives the ratio of the Michaelis constant to the maximum hydrolysis rate ( $K_m/V_{\max}$ ). For free urease  $K_m$  and  $V_{\max}$  are found to be  $1.1 \times 10^{-1}$  mol/l and  $1.0 \times 10^{-3}$  mol l<sup>-1</sup> s<sup>-1</sup>, respectively. In the case of immobilized enzyme the values of  $K_m$  and  $V_{\max}$  are found to be  $2.0 \times 10^{-1}$  mol/l and  $2.0 \times 10^{-4}$  mol l<sup>-1</sup> s<sup>-1</sup>, respectively. Kinetic data observed for immobilized urease is different from that of free urease. Kumar et al. observed the  $K_m$  value of immobilized urease on alginate bead was almost twice than that of free urease [39]. Increase in  $K_m$  and decrease in  $V_{\max}$  upon immobilization were observed for urease on polyurethane foam reported by Bachmeier et al. [40]. Godjevargova and Gabrovskaa reported  $V_{\max}$  for modified membranes was lower than that of free urease [41]. Our results show  $V_{\max}$  value for

free urease in solution is more compared to immobilized urease on nanoparticle. This is due to rate limitation imposed by diffusion. The apparent increase in  $K_m$  value after immobilization might be attributed due to changes in the accessibility of the substrate to the active sites of enzyme caused by diffusional limitations, steric effects and structural changes of enzyme after immobilization [42].

#### 4. Conclusion

In summary, nanosized carboxylic acid functionalized magnetic particles with high magnetic responsiveness and excellent dispersibility have been prepared through a facile one-pot synthesis and was successfully applied, for enzyme immobilization. The immobilized enzymes are reused more than 6 times without much degradation of activities. This investigation shows that the immobilized enzyme has activity not affected by wide change of pH, longer period of storage without losing catalytic activity and high thermal stability. These results are expected to open up a new possibility for the enzyme immobilization as well as a new application of magnetic nanoparticles. Immobilization of enzyme on magnetic nanoparticle offers several advantages compared to other conventional support because of easy product isolation by using a permanent magnet, low cost, facile preparation procedure and high chemical stability of enzyme on magnetic nanoparticle. This low cost route paves the way for immobilization of other industrially important enzymes easily. The key step in the enzymatic process lies in successful immobilization of the enzyme that allows for its recovery and reuse. The optimum pH and temperature profiles of the immobilized enzymes has compared to free form. The thermal stability of the urease was increased upon immobilization. This support is a promising material for storage and enzyme immobilization.

#### Acknowledgements

The authors gratefully acknowledge CSIR, New Delhi and DBT, Govt. of India for providing financial support for this work and Indian Institute of Technology, Kharagpur for execution of these studies.

#### References

- [1] M. Bystrzejewski, S. Cudzilo, A. Huczko, H. Lange, G. Soucy, G.C. Sanchez, W. Kaszuwara, *Biomol. Eng.* 24 (2007) 555–558.
- [2] J.M. Perez, F.J. Simeone, Y. Saeki, L. Josephson, R. Weissleder, *J. Am. Chem. Soc.* 125 (2003) 10192–10193.
- [3] J. Gao, H. Gu, A.B. Xu, *Acc. Chem. Res.* 42 (2009) 1097–1107.
- [4] A. Fornara, P. Johansson, K. Petersson, S. Gustafsson, J. Qin, E. Olsson, D. Ilver, A. Krozer, M. Muhammed, C. Johansson, *Nano Lett.* 8 (2008) 3423–3428.
- [5] P. Pouponneau, J.C. Leroux, S. Martel, *Biomaterials* 30 (2009) 6327–6332.
- [6] Y. Yong, Y. Bai, Y. Li, L. Lin, Y. Cui, C. Xia, *J. Magn. Magn. Mater.* 320 (2008) 2350–2355.
- [7] L. Wang, X. Gan, *Microchim. Acta* 164 (2009) 231–237.
- [8] Z. Shan, Q. Wua, X. Wang, Z. Zhou, K.D. Oakes, X. Zhang, Q. Huang, W. Yang, *Anal. Biochem.* 398 (2010) 120–122.
- [9] T.T. Baby, S. Ramaprabhu, *Talanta* 80 (2010) 2016–2022.
- [10] M.C. Urbina, S. Zinoveva, T. Miller, C.M. Sabliov, W.T. Monroe, C.S.S.R. Kumar, *J. Phys. Chem. C* 112 (2008) 11102–11108.
- [11] Y. Li, X. Li, J. Chu, C. Dong, J. Qi, Y. Yuan, *Environ. Pollut.* 158 (2010) 2317–2323.
- [12] L. Yu, I.A. Banerjee, X. Gao, N. Nuraje, H. Matsui, *Bioconjugate Chem.* 16 (2005) 1484–1487.
- [13] H.P.M.D. Hoog, I.W.C.E. Arends, A.E. Rowan, J.J.L.M. Cornelissen, R.J.M. Nolte, *Nanoscale* 2 (2010) 709–716.
- [14] T. Honda, M. Miyazaki, H. Nakamura, H. Maeda, *Chem. Commun.* 40 (2005) 5062–5064.
- [15] M. Tortajada, D. Ramon, D. Beltran, P. Amoros, *J. Mater. Chem.* 15 (2005) 3859–3868.
- [16] Y. Wang, F. Caruso, *Chem. Mater.* 17 (2005) 953–961.
- [17] S.S. Silva, R.A.S. Ferreira, L. Fu, L.D. Carlos, J.F. Mano, R.L. Reis, J. Rochad, *J. Mater. Chem.* 15 (2005) 3952–3961.
- [18] F.N. Serralha, J.M. Lopes, M.R. Aires-Barros, D.M.F. Prazeres, J.M.S. Cabral, F. Lemos, F.R. Ribeiro, *Enzyme Microb. Technol.* 31 (2002) 29–34.
- [19] A.X. Yan, X.W. Li, Y.H. Ye, *Appl. Biochem. Biotechnol.* 101 (2002) 113–129.
- [20] A. Vinu, M. Miyahara, K. Ariga, *J. Phys. Chem. B* 109 (2005) 6436–6441.
- [21] I.R.M. Tebeka, A.G.L. Silva, D.F.S. Petri, *Langmuir* 25 (2009) 1582–1587.
- [22] Y.Y. Liang, L.M. Zhang, *Biomacromolecules* 8 (2007) 1480–1486.
- [23] S.C. Tsang, C.H. Yu, X. Gao, K. Tam, *J. Phys. Chem. B* 110 (2006) 16914–16922.
- [24] G. Bayramoglu, H. Altunok, A. Bulut, A. Denizli, M.Y. Arica, *React. Funct. Polym.* 56 (2003) 111–121.
- [25] J. Laska, J. Włodarczyk, W. Zaborska, *J. Mol. Catal. B: Enzymatic* 6 (1999) 549–553.
- [26] M. Senel, A. Coskun, M.F. Abasiyanik, A. Bozkurt, *Chem. Pap.* 64 (2010) 1–7.
- [27] J.P. Chen, S.H. Chiu, *Enzyme Microb. Technol.* 26 (2000) 359–367.
- [28] A. Dyal, K. Loos, M. Noto, S.W. Chang, C. Spagnoli, K.V.P.M. Shafi, A. Ulman, M. Cowman, R.A. Gross, *J. Am. Chem. Soc.* 125 (2003) 1684–1685.
- [29] Y. Zhu, S. Kaskel, J. Shi, T. Wage, K.H. van Pee, *Chem. Mater.* 19 (2007) 6408–6413.
- [30] T. Kuroiwa, Y. Noguchi, M. Nakajima, S. Sato, S. Mukataka, S. Ichikawa, *Process Biochem.* 43 (2008) 62–69.
- [31] W. Xie, N. Ma, *Energy Fuels* 23 (2009) 1347–1353.
- [32] M. Das, D. Mishra, P. Dhak, S. Gupta, T.K. Maiti, A. Basak, P. Pramanik, *Small* 5 (2009) 2883–2893.
- [33] S. Mohapatra, P. Pramanik, *Colloids Surf., A* 339 (2009) 35–42.
- [34] M. Das, D. Mishra, T.K. Maiti, A. Basak, P. Pramanik, *Nanotechnology* 19 (2008) 415101–415115.
- [35] S. Mohapatra, N. Pramanik, S. Mukherjee, S.K. Ghosh, P. Pramanik, *J. Mater. Sci.* 42 (2007) 7566–7574.
- [36] M.S. Rao, M. Chellapandian, M.R.V. Krishnan, *Bioprocess. Eng.* 13 (1995) 211–214.
- [37] K. Gabrovska, A. Georgieva, T. Godjevargova, O. Stoilova, N. Manolova, *J. Biotechnol.* 129 (2007) 674–680.
- [38] M. Tortajada, D. Ramon, D. Beltrand, P. Amoros, *J. Mater. Chem.* 15 (2005) 3859–3868.
- [39] S. Kumar, A. Dwevedi, A.M. Kayastha, *J. Mol. Catal. B: Enzymatic* 58 (2009) 138–145.
- [40] K.L. Bachmeier, A.E. Williams, J.R. Warmington, S.S. Bang, *J. Biotechnol.* 93 (2002) 171–181.
- [41] T. Godjevargova, K. Gabrovska, *Enzyme Microb. Technol.* 38 (2006) 338–342.
- [42] S. Mulagalapalli, S. Kumar, R.C.R. Kalathur, A.M. Kayastha, *Appl. Biochem. Biotechnol.* 142 (2007) 291–297.